 Related Commentary, page 760

Inhibition of 11β–hydroxysteroid dehydrogenase type II selectively blocks the tumor COX-2 pathway and suppresses colon carcinogenesis in mice and humans

Ming-Zhi Zhang,[1,2] Jie Xu,[1] Bing Yao,[1] Huiyong Yin,[1] Qiuyin Cai,[1] Martha J. Shrubsole,[1] Xiwu Chen,[1] Valentina Kon,[3] Wei Zheng,[1] Ambra Pozzi,[1] and Raymond C. Harris[1]

[1]Department of Medicine, [2]Department of Cancer Biology, and [3]Department of Pediatrics, Vanderbilt University School of Medicine, Nashville, Tennessee, USA.

Colorectal cancer (CRC) is a leading cause of cancer death, yet primary prevention remains the best approach to reducing overall morbidity and mortality. Studies have shown that COX-2–derived PGE_2 promotes CRC progression, and both nonselective COX inhibitors (NSAIDs) and selective COX-2 inhibitors (such as glucocorticoids) reduce the number and size of colonic adenomas. However, increased gastrointestinal side effects of NSAIDs and increased cardiovascular risks of selective COX-2 inhibitors limit their use in chemoprevention of CRC. We found that expression of 11β–hydroxysteroid dehydrogenase type II (11βHSD2), which converts active glucocorticoids to inactive keto-forms, increased in human colonic and *Apc*$^{+/min}$ mouse intestinal adenomas and correlated with increased COX-2 expression and activity. Furthermore, pharmacologic inhibition or gene silencing of 11βHSD2 inhibited COX-2–mediated PGE_2 production in tumors and prevented adenoma formation, tumor growth, and metastasis in mice. Inhibition of 11βHSD2 did not reduce systemic prostacyclin production or accelerate atherosclerosis in mice, thereby avoiding the major cardiovascular side effects seen with systemic COX-2 inhibitors. Therefore, 11βHSD2 inhibition represents what we believe to be a novel approach for CRC chemoprevention and therapy by increasing tumor glucocorticoid activity, which in turn selectively blocks local COX-2 activity.

Introduction

Colorectal cancer (CRC) is a leading cause of cancer death. COX-2–derived PGE_2 promotes CRC progression (1), and inhibition of COX-2–derived PGE_2 production by traditional NSAIDs or selective COX-2 inhibitors reduces the number and size of adenomas in familial adenomatous polyposis (FAP) patients and in mice with an autosomal-dominant heterozygous nonsense mutation of the mouse gene encoding adenomatous polyposis coli (*Apc*$^{+/min}$ mice; refs. 2–7). However, increased gastrointestinal side effects of traditional NSAIDs and increased cardiovascular risks of selective COX-2 inhibitors limit their utility in chemoprevention of CRC (8, 9).

Glucocorticoids mediate their antiinflammatory effects in part by inhibiting PG production. Unlike NSAIDs, which suppress PGE_2 production by inhibition of COX enzymatic activity, glucocorticoids inhibit multiple steps in the PG cascade: inhibiting cytosolic phospholipase A_2 ($cPLA_2$) activity, which releases the COX substrate arachidonic acid, and inhibiting expression of both COX-2 and microsomal PGE synthase (mPGES-1), the terminal enzyme of COX-2–mediated PGE_2 biosynthesis (10, 11). In addition to treatment of hematologic malignancies, glucocorticoids can inhibit solid tumor growth, regress tumor mass, and prevent metastasis by blocking angiogenesis (12–14). However, the undesirable side effects of immune suppression limit their application in cancer chemoprevention and chemotherapy.

In cultured cells, COX-2 expression and PGE_2 production can be suppressed by glucocorticoids at concentrations as low as 10^{-9} M (15). Because levels of circulating glucocorticoids are approximately 10^{-6} to 10^{-7} M (cortisol in humans and corticosterone [CS] in rodents), COX-2 expression might be expected to be tonically suppressed by circulating glucocorticoids; however, COX-2 is constitutively expressed in human colonic adenomas and in *Apc*$^{+/min}$ mouse intestinal adenomas (5, 16). Normally, 11β–hydroxysteroid dehydrogenase type II (11βHSD2) inactivates intracellular glucocorticoids in the classic mineralocorticoid-responsive organs, kidney and intestine (particularly colon), in order to maintain the specificity of the mineralocorticoid receptor to activation by aldosterone (17). We have previously shown that pharmacologic inhibition of 11βHSD2 activity suppresses kidney cortex COX-2 expression by elevating intracellular levels of endogenous active glucocorticoids (18). In the present study, we determined that 11βHSD2 expression increased in parallel to COX-2 expression and activity in colonic adenomas. Furthermore, either genetic or pharmacologic inhibition of 11βHSD2 led to decreased COX-2 expression and activity in colonic adenomas and tumors and significantly suppressed adenoma and tumor growth. These findings suggest an important role for 11βHSD2 in regulation of COX-2 expression in colonic tumors and identify 11βHSD2 as a possible target for prevention and/or therapy of colorectal cancer.

Results

Increased 11βHSD2 in colonic adenomas. In human colonic adenomas, 11βHSD2 mRNA levels increased significantly compared

Conflict of interest: The authors have declared that no conflict of interest exists.

Nonstandard abbreviations used: cPGES, cytosolic PGE synthase; $cPLA_2$, cytosolic phospholipase A_2; CRC, colorectal cancer; CS, corticosterone; FAP, familial adenomatous polyposis; GA, glycyrrhizic acid; GE, glycyrrhetinic acid; 11βHSD2, 11β–hydroxysteroid dehydrogenase type II; mPGES-1, microsomal PGE synthase; PGI_2, prostacyclin.

Citation for this article: *J. Clin. Invest.* **119**:876–885 (2009). doi:10.1172/JCI37398.

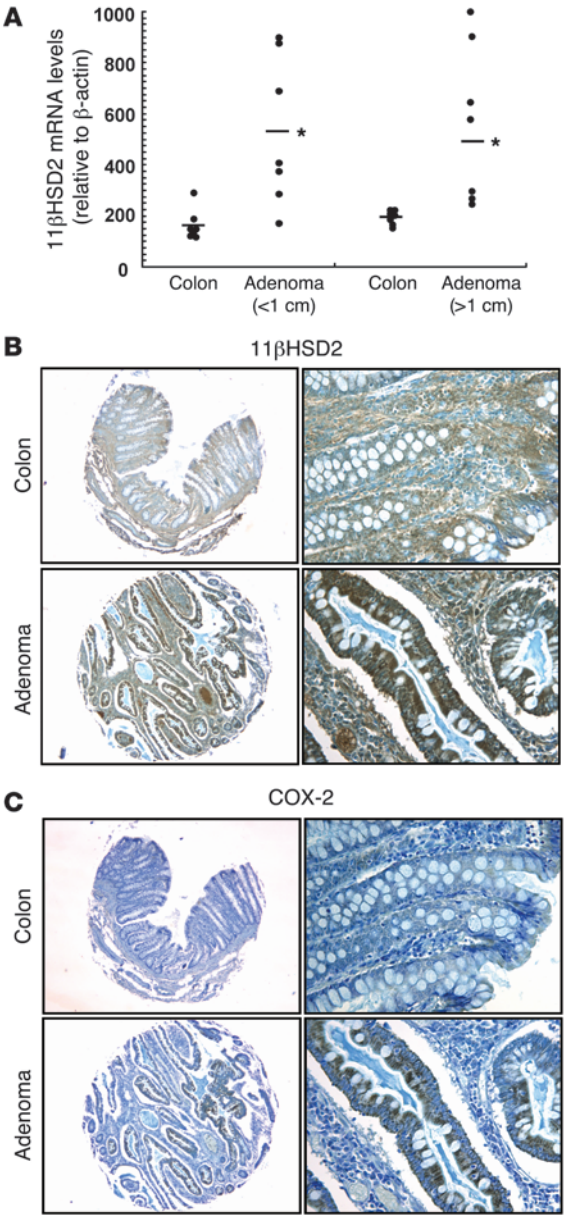

Figure 1
Increased expression of 11βHSD2 and COX-2 in human colonic adenomas. (**A**) Levels of 11βHSD2 mRNA increased in both small and large adenomas compared with corresponding normal colonic tissues. Data points denote levels in individual patients (n = 7 per group) as determined by real-time PCR; horizontal bars indicate mean expression within each group. *P < 0.01 versus normal tissue. (**B**) Representative photomicrographs indicated increased 11βHSD2 expression in the stroma and epithelium in human colonic adenomas compared with normal colonic tissues. (**C**) Representative photomicrographs indicated increased COX-2 expression in the epithelial cells of human colonic adenomas compared with normal colonic tissues. Original magnification, ×25 (left); ×160 (right).

with levels in normal colonic tissues (Figure 1A). Protein expression of 11βHSD2 increased in both epithelia and stroma in all human colonic adenomas investigated (Figure 1B). Quantitative image analysis showed significant increases in 11βHSD2 expression in adenomas compared with normal colonic tissues (11βHSD2 area/tissue area, adenoma, 0.125 ± 0.029; normal tissue, 0.019 ± 0.005; P < 0.01, n = 6). COX-2 and 11βHSD2 expression increased coordinately in colonic adenoma epithelial cells compared with normal colonic tissue (Figure 1, B and C). Increased stromal COX-2 expression was only detected in a subset of adenomas (Supplemental Figure 1).

Glucocorticoid-induced inhibition of CT26 cell COX-2 expression attenuated by 11βHSD2 activity. Mouse colon adenocarcinoma CT26 cells constitutively express COX-2. In CT26 cells overexpressing 11βHSD2 after transfection of 11βHSD2 cDNA (Figure 2A), COX-2 expression under basal conditions was similar to that in CT26 cells transfected with an empty vector. However, treatment with a high concentration of CS (1,000 nM) for 16 h significantly inhibited COX-2 expression in vector-transfected CT26 cells, but minimally inhibited COX-2 expression in the 11βHSD2-overexpressing cells. Administration of the 11βHSD2 inhibitor glycyrrhizic acid (GA) did enhance CS-induced COX-2 inhibition in the 11βHSD2-overexpressing cells (Figure 2B).

Pharmacologic inhibition of 11βHSD2 suppressed adenoma COX-2 expression and growth in $Apc^{+/min}$ mice. In $Apc^{+/min}$ mouse samples, increased expression of COX-2 and 11βHSD2 was evident in both adenoma stroma and epithelia and at the junction of tumor and normal tissue (Figure 3A). Administration of GA to $Apc^{+/min}$ mice for 8 wk significantly reduced total adenoma number and size as well as adenoma COX-2 and mPGES-1 expression (Figure 3, B–D).

Inhibition of 11βHSD2 blocked colonic adenocarcinoma tumor growth by activation of glucocorticoid receptors. Because GA, the major bioactive triterpene glycoside of licorice root extracts, has other potential targets in addition to 11βHSD2, we used shRNA to knock down 11βHSD2 in CT26 cells. Knocking down 11βHSD2 in 2 independent clones ($CT26^{shRNA3-31}$ and $CT26^{shRNA2-9}$; Figure 4A) inhibited 11βHSD2 activity more potently than did 10 μM GA (control CT26, 40.96 ± 8.96 pmol/h/mg protein; CT26 plus GA, 22.10 ± 0.41 pmol/h/mg protein; $CT26^{shRNA3-31}$, 14.44 ± 1.27 pmol/h/mg protein; $CT26^{shRNA2-9}$, 12.57 ± 0.62 pmol/h/mg protein; P < 0.01, CT26 plus GA versus CT26, and each knockdown versus both CT26 and CT26 plus GA; n = 4; Supplemental Figure 2A). Knocking down 11βHSD2 significantly enhanced low-dose CS–induced (10 nM) inhibition of CT26 cell COX-2 expression (Figure 4B and Supplemental Figure 2B), PGE_2 production (Figure 4C), and cell migration (Supplemental Figure 3A). Knocking down 11βHSD2 reduced tumor size (Figure 4D) and number (Table 1) and decreased tumor COX-2 and mPGES-1 expression (Figure 4E). Therefore, selective inhibition of 11βHSD2 activity led to suppression of tumor COX-2 expression and growth.

Similar to 11βHSD2 knockdowns, pharmacologic inhibition of11βHSD2 activity with GA significantly enhanced low-dose CS–mediated inhibition of CT26 cell COX-2 expression (Figure 5A) and cell migration, to the same extent as a selective COX-2 inhibitor (Supplemental Figure 3B). GA also substantially reduced tumor COX-2 and PGE_2 levels as well as tumor growth (Figure 5B) and number (Table 1). Inhibition of tumor growth was dose dependent, with maximal inhibition achieved at a GA concentration of 3 mg/kg/d (Supplemental Figure 4A), which is comparable to doses that have been safely administered to humans in long-term studies (19, 20). GA treatment also led to significant decreases in phosphorylated $cPLA_2$ and mPGES-1

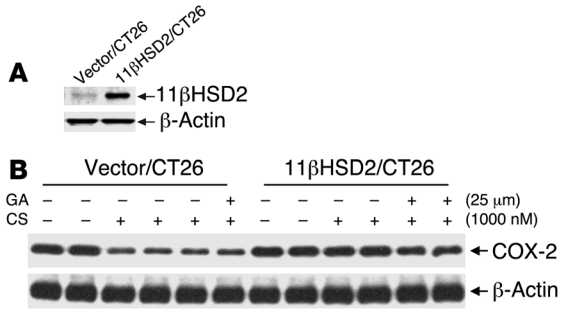

Figure 2
Overexpression of 11βHSD2 attenuated CS-induced COX-2 inhibition in CT26 cells. (**A**) Increased 11βHSD2 protein expression in CT26 cells 72 h after transfection with pCMV-SPORT6 containing the entire open reading frame of mouse 11βHSD2 cDNA. (**B**) Treatment with 1,000 nM CS for 16 h markedly inhibited COX-2 expression in CT26 cells transfected with empty vector, but not in 11βHSD2-overexpressing CT26 cells. The 11βHSD2 inhibitor GA partly restored CS-induced COX-2 inhibition in 11βHSD2-overexpressing CT26 cells.

expression in tumors (Figure 5C). However, GA treatment had no effect on the expression of COX-1 or cytosolic PGE synthase (cPGES), a terminal enzyme in COX-1–mediated PGE_2 biosynthesis (Figure 5C). The glucocorticoid receptor antagonist RU486 completely reversed GA inhibition of tumor COX-2 expression, PGE_2 biosynthesis, and growth (Figure 5B), which indicates that glucocorticoid receptor activation mediated GA-induced inhibition of both COX-2 activity and CT26 tumor growth. GA treatment led to significant increases in CS levels with concomitant decreases in levels of the inactive CS metabolite 11-keto-corticosterone in kidney, colon, and tumors (Figure 5D). Most GA was found to be converted to its more active metabolite, glycyrrhetinic acid (GE), at 24 h after the last administration of GA (Supplemental Figure 5 and ref. 21). Furthermore, in CT26-derived tumors, GA had no additive effect on growth inhibition by the selective COX-2 inhibitor SC58236 (2 mg/kg/d i.p.; Supplemental Figure 4B). Therefore, COX-2 inhibition was an essential step in GA-mediated tumor suppression.

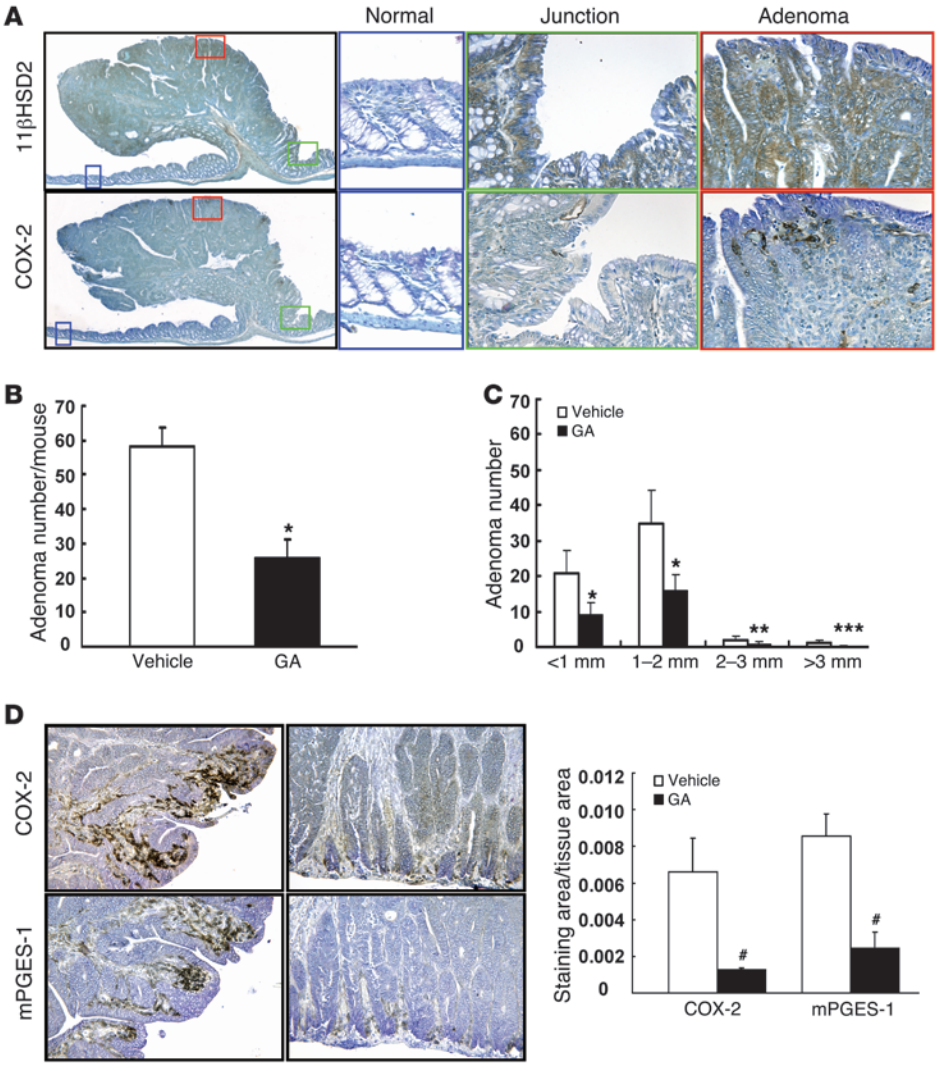

Figure 3
Increased expression of COX-2 and 11βHSD2 in *Apc*$^{+/min}$ mouse intestinal adenomas. (**A**) Representative photomicrographs indicated increased COX-2 and 11βHSD2 expression in the stroma and epithelium in the adenomas and at the junction of normal tissue and adenoma in *Apc*$^{+/min}$ mice. Blue, green, and red boxed regions are shown at higher magnification, denoted by corresponding outlines. Original magnification, ×20 (whole adenoma); ×160 (high-magnification views). (**B** and **C**) Inhibition of 11βHSD2 activity with GA (30 mg/kg/d i.p.) reduced *Apc*$^{+/min}$ mouse intestinal adenoma multiplicity (n = 12 per group) and size. (**D**) GA inhibited *Apc*$^{+/min}$ mouse adenoma COX-2 and mPGES-1 expression. n = 4 per group. Original magnification, ×100. $^{*}P < 0.0001$, $^{**}P < 0.005$, $^{***}P < 0.02$, $^{\#}P < 0.01$ versus vehicle.

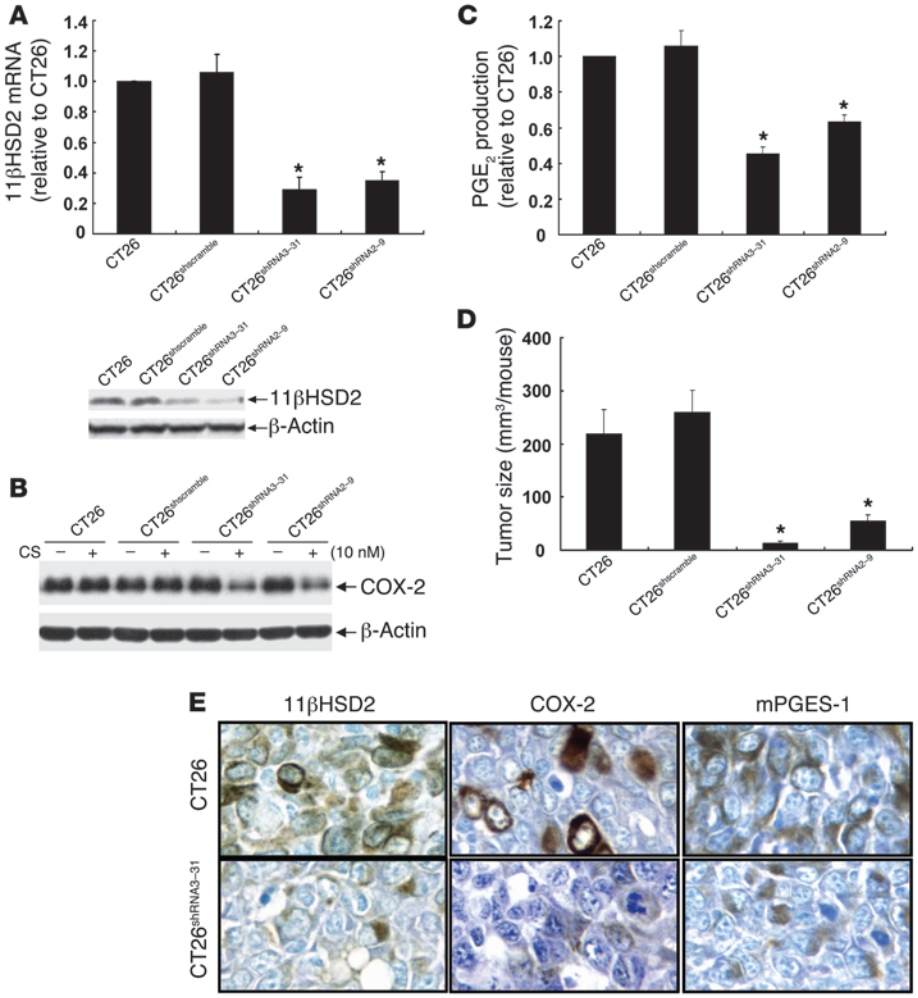

Figure 4
Knockdown of 11βHSD2 suppressed CT26 tumor growth. (**A**) Protein and mRNA levels of 11βHSD2 were reduced in $CT26^{shRNA3–31}$ and $CT26^{shRNA2–9}$ cells, but not in $CT26^{shscramble}$ cells. $n = 3$. (**B** and **C**) Knockdown of 11βHSD2 augmented low-dose CS–induced inhibition of CT26 cell COX-2 expression (**B**) and PGE_2 production (**C**). $n = 4$. (**D**) Tumor growth was significantly reduced in tumors derived from 11βHSD2 knockdown $CT26^{shRNA3–31}$ cells and $CT26^{shRNA2–9}$ cells. $n = 6$. (**E**) Representative photomicrographs demonstrate reduced 11βHSD2, COX-2, and mPGES-1 expression in tumors derived from 11βHSD2 knockdown $CT26^{shRNA3–31}$ cells. Original magnification, ×400. *$P < 0.0001$ versus CT26.

Human colon carcinoma HCA-7 cells constitutively expressed both 11βHSD2 and COX-2 (Supplemental Figure 6A), and COX-2 activity is essential for the proliferation of HCA-7 cells (22). Compared with HCA-7 cells, human colon carcinoma HT-29 cells constitutively expressed similar levels of 11βHSD2 but had minimal COX-2 expression (Supplemental Figure 6A), and COX-2 activity is not essential for HT-29 cell proliferation (23). As indicated in Supplemental Figure 6B, proliferation of HCA-7 cells, but not HT-29 cells, was inhibited by treatment with selective COX-2 inhibition with SC58236 or NS-398. GA treatment had no effect on HT-29–derived tumor growth (Supplemental Figure 6C). In contrast, GA inhibited COX-2 and mPGES-1 expression in HCA-7–derived tumors and significantly blocked tumor growth (Supplemental Figure 6D).

Inhibition of 11βHSD2 blocked angiogenesis and colonic adenocarcinoma metastasis. Metastasis is the major cause of death in CRC. Glucocorticoids can limit CRC hepatic metastasis by inhibiting angiogenesis (12, 13). VEGF plays a key role in tumor-associated angiogenesis, and COX-2–derived PGE_2 promotes angiogenesis via stimulation of VEGF expression (24). GA treatment dramatically reduced CT26 tumor VEGF expression (Supplemental Figure 7A) and tumor blood vessel density (Supplemental Figure 7B). The effects of GA or 11βHSD2 knockdown on metastasis were investigated in the tail vein injection model (25). Compared with mice injected with wild-type CT26 or $CT26^{shscramble}$ cells (see Methods for details of cell line generation), mice injected with $CT26^{shRNA3–31}$ or $CT26^{shRNA2–9}$ cells and mice injected with CT26 cells plus GA demonstrated decreased lung tumor COX-2 and mPGES-1 expression (Figure 6B) as well as decreased lung tumor number and size (Figure 6A), which was associated with increased survival time (Figure 6C).

Inhibition of 11βHSD2 did not alter systemic PG production or promote atherogenesis. Although clinical trials have indicated that selective COX-2 inhibitors reduce colon adenoma formation in patients at high risk for CRC, these trials also highlighted the increased car-

Table 1
Effects of GA and 11βHSD2 knockdown on CT26 tumor incidence

Treatment group	Tumor incidence (*n*)					*P*[A]
	0%	25%	50%	75%	100%	
Vehicle ($n = 19$)	0	1	0	9	9	–
GA ($n = 20$)	2	3	7	8	0	<0.0001
11βHSD2 knockdown ($n = 19$)	5	7	5	2	0	<0.0001

For vehicle- and GA-treated groups, data from different experiments were combined; the 11βHSD2 knockdown group shows data from $CT26^{sh/RNA3–31}$- and $CT26^{sh/RNA2–9}$-injected mice. [A]Compared with vehicle.

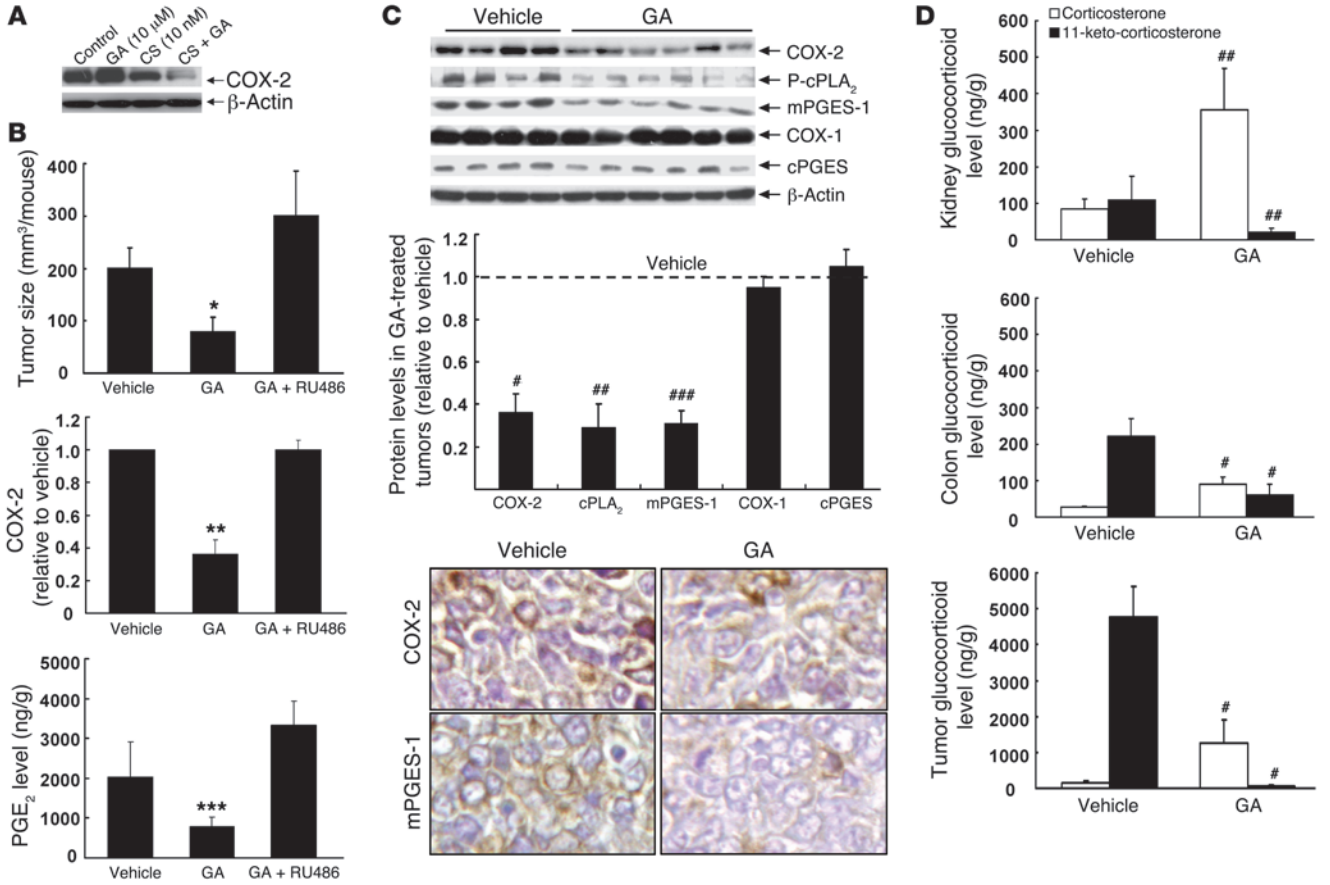

Figure 5

Inhibition of 11βHSD2 activity with GA suppressed tumor growth through activation of glucocorticoid receptors. (**A**) GA augmented low-dose CS–induced inhibition of CT26 cell COX-2 expression. (**B**) Treatment with 10 mg/kg/d GA i.p. led to significant decreases in tumor size, COX-2 expression, and PGE_2 levels, which were completely reversed by the glucocorticoid receptor inhibitor RU486 (7.5 mg/kg/d i.m.). n = 5–6 per group. (**C**) GA reduced CT26 tumor expression of phosphorylated $cPLA_2$ (P-$cPLA_2$) and mPGES-1, but had no effect on tumor expression of COX-1 (P = 0.23) and cPGES (P = 0.055). Original magnification, ×400. (**D**) GA treatment significantly increased corticosterone levels and decreased 11-keto-corticosterone levels in kidney, colon, and tumors. n = 5. $^{*}P < 0.0001$, $^{**}P < 0.001$, $^{***}P < 0.02$, $^{\#}P < 0.05$, $^{\#\#}P < 0.01$, and $^{\#\#\#}P < 0.005$ versus vehicle.

diovascular risk engendered by these agents (8, 26). Selective COX-2 inhibitors suppress endothelial COX-2–derived prostacyclin (PGI_2) production without inhibition of COX-1–mediated prothrombotic platelet thromboxane A_2 production, which increases the propensity for thrombogenesis and atherogenesis (27). Administration of COX-2 inhibitors to mice decreases urinary levels of the major PGI_2 metabolite, 2,3-dinor-6-keto $PGF_{1\alpha}$ (28). In contrast, administration of GA for 1 mo at concentrations up to 30 mg/kg/d did not inhibit urinary 2,3-dinor-6-keto $PGF_{1\alpha}$ excretion or alter urinary 2,3-dinor thromboxane B_2 excretion (Supplemental Figure 8A). Furthermore, in female apoE-null mice, a model of spontaneous atherosclerosis that recapitulates many features of human atherosclerosis (29), GA treatment (10 mg/kg/d i.p.) for 10 wk did not accelerate progression of atherosclerosis (Supplemental Figure 8B). GA treatment did not alter systolic blood pressure, and serum potassium was unchanged in mice administered concentrations of GA up to 30 mg/kg/d (data not shown). Therefore, in this model, chronic use of GA at tumor-suppressive concentrations did not induce the cardiovascular side effects previously reported with selective COX-2 inhibitors (8, 26).

Discussion

Our present results indicate that tissue 11βHSD2 activity contributes to increased COX-2 expression in colorectal tumors and that inhibition of 11βHSD2 activity in vivo suppresses COX-2–derived PGE_2 production and colorectal tumor growth as a result of increased intracellular active glucocorticoids (Figure 7). Recent studies have demonstrated a molecular link between COX-2–derived PGE_2 and CRC progression (1). Clinical evidence indicates a 40%–50% reduction in CRC in individuals taking NSAIDs regularly, either in the context of sporadic CRC or in FAP patients (3, 30–32). However, long-term use of traditional NSAIDs increases gastrointestinal side effects. Reports estimate 10,000–20,000 deaths and 100,000 hospitalizations per year in the United States related to gastrointestinal complications induced by traditional NSAIDs (33). The antiinflammatory properties of NSAIDs are attributed to COX-2 inhibition, while their gastrointestinal side effects are attributed predominantly to COX-1 inhibition (6, 7, 34).

Selective COX-2 inhibitors have shown efficacy similar to that of traditional NSAIDs in treating acute and chronic inflammatory conditions and in reducing the number and size of adenomas

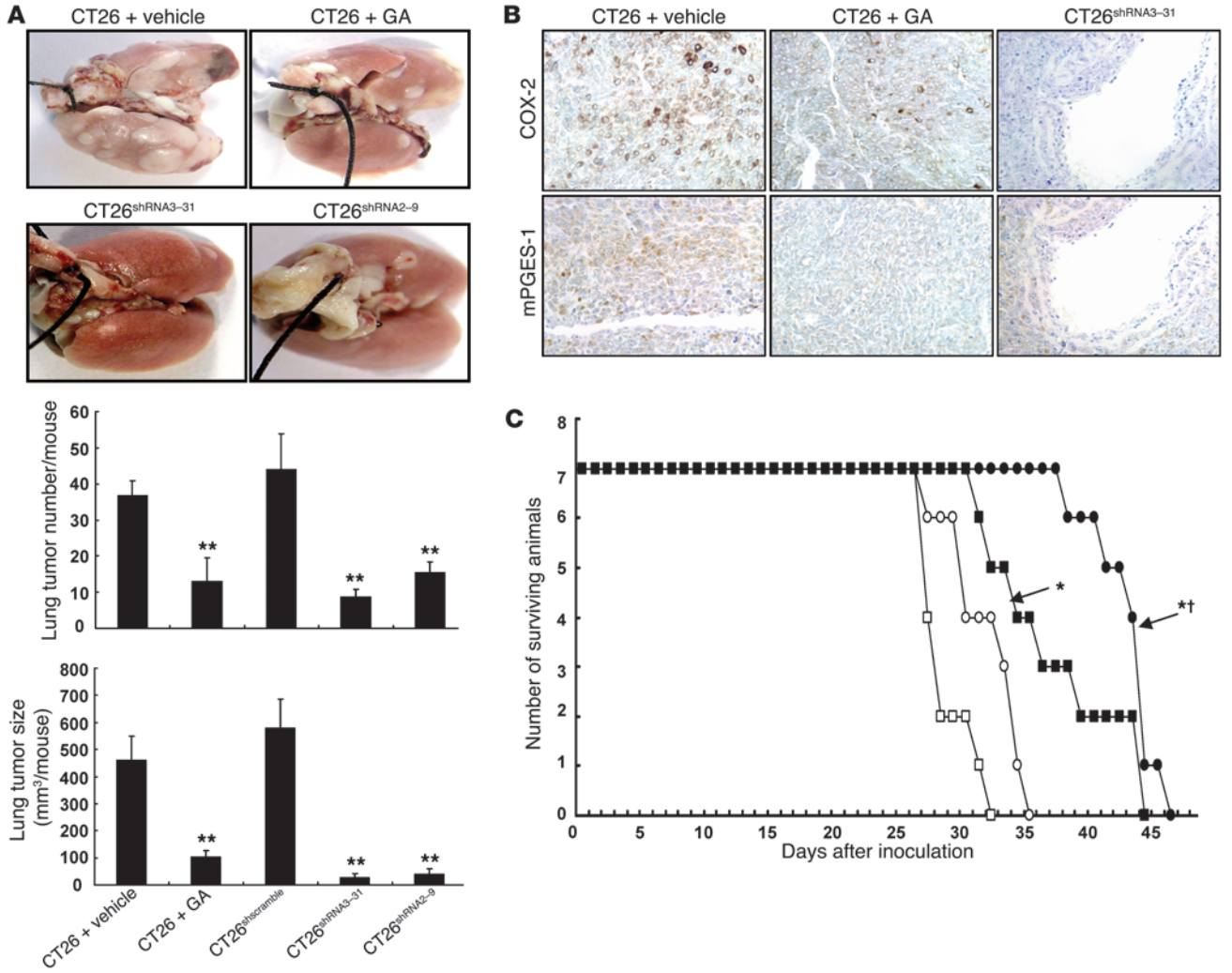

Figure 6

Pharmacologic or genetic inhibition of 11βHSD2 activity suppressed CT26 tumor metastasis. (**A**) Either treatment with 10 mg/kg/d GA i.p. or 11βHSD2 knockdown inhibited metastatic lung tumor number and growth induced by tail vein injection of CT26 cells. $n = 6$. (**B**) Either treatment with GA or 11βHSD2 knockdown reduced COX-2 and mPGES-1 expression in metastatic lung tumors. Original magnification, ×160. (**C**) Either treatment with GA (filled squares) or 11βHSD2 knockdown (filled circles) increased the survival of mice receiving tail vein injections of CT26 cells. $n = 7$. Control CT26^{shscramble} and CT26 groups are shown by open squares and open circles, respectively. *$P < 0.05$, **$P < 0.0001$ versus wild-type CT26; †$P < 0.05$ versus GA; ANOVA and post-hoc test.

in FAP patients and *Apc*$^{+/min}$ mice, with fewer gastrointestinal side effects (2, 4, 5). Therefore, COX-2 inhibitors were touted as promising agents for chemoprevention and chemotherapy of CRC. It has been suggested that the increased incidence of cardiovascular events associated with long-term use of selective COX-2 inhibitors is caused by the selective inhibition of COX-2–derived PGI_2 production in endothelial cells (8, 9). Since platelets express only COX-1, COX-2 inhibition will not inhibit the production of COX-1–mediated prothrombotic platelet thromboxane A_2 (27). In the current study, long-term treatment with a selective 11βHSD2 inhibitor did not promote atherogenesis in a mouse proatherogenic model, unlike what has been previously described with COX-2 inhibitors (35).

The physiological function of 11βHSD2 is to inactivate glucocorticoids, thereby preventing glucocorticoid-induced activation of mineralocorticoid receptors in aldosterone-responsive tissues such as the kidney and colon (15, 36). Inhibition of 11βHSD2 significantly inhibited CS metabolism and thereby increased levels of active glucocorticoid in colonic tumor (Figure 5D). Glucocorticoids are known to inhibit cell proliferation and induce cell differentiation through activation of glucocorticoid receptors. Although glucocorticoids have previously been used to treat certain hematological malignancies (37) and have been reported to inhibit the growth of colon cancer cell lines and to inhibit CRC hepatic metastasis (12, 13), systemic administration of glucocorticoids is not suitable for chemoprevention and chemotherapy of CRC because of immunosuppression and other systemic side effects.

Recently, the potential role of 11βHSD2 in tumorigenesis has attracted interest. Expression of 11βHSD2 increases in some tumors and tumor cell lines (38–40). In MCF-7 breast cancer cells,

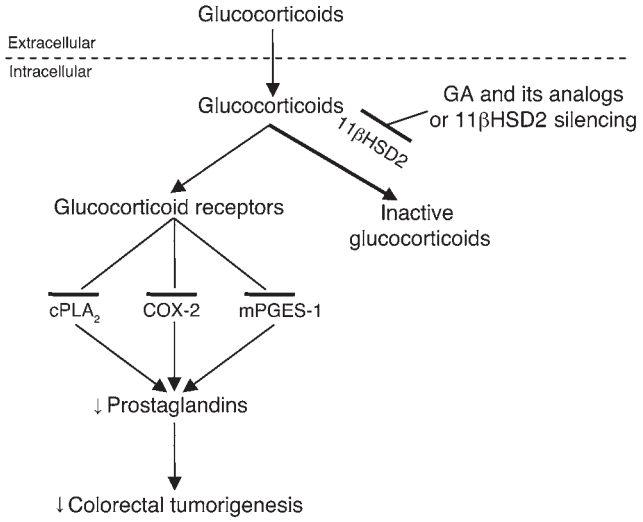

Figure 7
Proposed mechanism underlying 11βHSD2 activity and colorectal tumorigenesis. In tumor cells, glucocorticoids are converted to inactive keto-forms by 11βHSD2, reducing glucocorticoid receptor activation, while inhibition of 11βHSD2 activity (by GA and its analogs or by gene knockdown) leads to increased levels of intracellular active glucocorticoids. The consequent inhibition of $cPLA_2$ activity and COX-2 and mPGES-1 expression results in blockade of PGE_2 production and inhibition of tumor growth.

glucocorticoid-induced inhibition of cell proliferation is attenuated by 11βHSD2 (41). The results of the present study indicate that a major mechanism for an antitumor effect of 11βHSD2 inhibition in colonic adenomas and carcinomas is the inhibition of COX-2 expression and production of COX-2–dependent PGs by increasing local concentrations of glucocorticoids, and that this COX-2 inhibition will markedly inhibit tumorigenesis.

We propose that inhibition of 11βHSD2 activity may provide a new target for chemoprevention and/or adjunctive therapy for CRC, particularly for patients with increased risk, such as FAP patients, because of the following advantages. First, selectively decreased COX-2, but not COX-1, mediated PG production. Therefore, inhibition of 11βHSD2 activity has the beneficial effects of traditional NSAIDs to prevent and regress CRC without the gastrointestinal side effects associated with COX-1 inhibition. Second, physiologic 11βHSD2 expression is largely restricted to colon and kidney. Therefore, inhibition of 11βHSD2 activity is not expected to incur the cardiovascular risk posed by COX-2 inhibitors that suppress COX-2–derived PGI_2 production in vascular endothelial cells. Finally, increased levels of intracellular active glucocorticoids were observed only in tissues with elevated levels of 11βHSD2 expression. Inhibition of 11βHSD2 will not produce immunosuppression or other systemic side effects of conventional glucocorticoid therapy. It is also possible that increased intracellular active endogenous glucocorticoids may also inhibit colorectal tumorigenesis through non–PG-mediated pathways, such as stimulation of p53-dependent pathways (42).

Tissue PG levels are determined by both biosynthesis and catabolism. A key enzyme in PG catabolism, 15-hydroxyprostaglandin dehydrogenase, has been reported to decrease in human colorectal cancer and in $Apc^{+/min}$ mouse intestinal adenomas (43). Studies have indicated that glucocorticoids can induce 15-hydroxyprostaglandin in A549 human lung adenocarcinoma cells (44). Therefore, it is possible that increased intracellular active endogenous glucocorticoids may inhibit colorectal tumorigenesis not only by inhibiting PG synthesis, but also by enhancing PG degradation.

GA and its analogs are excellent prototypes for 11βHSD2 inhibitors. GA is a natural compound contained in licorice, a natural botanical antiinflammatory agent and a powerful 11βHSD2 inhibitor. Long-term excessive ingestion of licorice has been reported to induce hypokalemia and elevation of blood pressure in a subset of people (20). Although these side effects were not seen with GA treatment in our experimental animals, nor have they been reported as a substantial limitation in studies of humans treated daily with comparable doses of GA for extended periods (19, 45), we did observe that the concentrations of GA used in our studies increased levels of active CS in the kidney (Figure 5D). Therefore, it is likely that if comparable doses of GA were used in humans, some percentage of patients would develop hypertension and/or hypokalemia, requiring treatment with the potassium-sparing diuretic amiloride. However, the need to monitor for these potential side effects should not necessarily preclude the use of 11βHSD2 inhibition as a strategy to inhibit colorectal tumor COX-2 expression and growth.

Methods

$Apc^{+/min}$ mouse model. The germline mutations in the *APC* gene lead to FAP, and inactivation of APC is also found in most sporadic colorectal cancers (5). $Apc^{+/min}$ mice have an autosomal-dominant heterozygous nonsense mutation of the mouse *Apc* gene, homologous to human germline and somatic *APC* mutations, and develop adenomas to a grossly detectable size within a few months. Male $Apc^{+/min}$ mice (5 wk old) were obtained from The Jackson Laboratory and treated with either vehicle (water) or GA (30 mg/kg/d i.p.) for 8 wk. Under anesthesia with Nembutal (60 mg/kg i.p.; Abbot Laboratories), the entire intestine was dissected, flushed thoroughly with ice-cold PBS (pH 7.4), and then filled with fixative (15). The intestine was transferred to 70% ethanol for 24 h, opened longitudinally, and examined using a dissecting microscope to count polyps in a blinded fashion. The tumor diameter was measured with a digital caliper. After tumors were counted, intestinal tissues were processed for paraffin embedding. All animal experiments were performed according to animal care guidelines and were approved by the Vanderbilt University IACUC.

Primary tumor growth. For mouse adenocarcinoma CT26 tumor experiments, male BALB/c mice (8 wk old; 18–20 g) were given 4 dorsal s.c. injections of CT26 cells (5×10^5 cells per site), as previously described (46), with administration of either vehicle (water, i.p. daily) or different doses of GA (1–30 mg/kg/d i.p.) begun 1 d prior to cell injection. Tumors were harvested after 18 d of growth and evaluated for tumor incidence — scored as 100% if 4 tumors developed, 75% if 3 tumors developed, and so on — and tumor volume (expressed in mm^3 and calculated as $[l \times w^2] \times 0.5$, where l and w denote length and width, respectively; ref. 47). For human colon carcinoma experiments, athymic nude mice (8 wk old; Harlan Sprague Dawley) were given 4 dorsal s.c. injections of HCA-7 cells (3.35×10^6 cells per site) or HT-29 cells (4.5×10^6 cells per site), with administration of either vehicle (water) or GA (10 mg/kg/d i.p.) begun 1 d prior to cell injection. Tumor sizes were measured by external measurement (47).

Metastatic tumor growth. Male BALB/c mice (8 wk old; 18–20 g) received a single tail vein injection of wild-type CT26 cells or 11βHSD2 knockdown CT26 cells (2.5×10^4 cells in 0.5 ml medium). Mice receiving CT26 cells were administered vehicle (water) or GA (10 mg/kg/d i.p.) initiated 1 d prior to cell injection. We sacrificed 6 mice from each group 4 wk after injection and kept the remaining mice until death to generate survival

curves. The lungs were removed, weighed, and fixed in fixative or kept in PBS, after which the metastatic lung tumors were counted and tumor volumes measured as described above (47).

GA and blood pressure and atherosclerosis in Apoe$^{-/-}$ mice. Female *Apoe*$^{-/-}$ mice on the C57BL/6 background were obtained from The Jackson Laboratory. The mice were fed a high-fat diet (0.2% cholesterol, 21% saturated fat, formula TD88173; Harlan Teklad) from 6 wk of age and treated with vehicle (water) or GA (10 mg/kg/d, i.p.) for 10 wk. Blood pressure was measured by tail-cuff method 1 wk before sacrifice. Under anesthesia with Nembutal (60 mg/kg i.p.; Abbot Laboratories), the hearts and proximal aortae were dissected and placed in formalin, paraffin embedded, and cut (10 μm) serially from the proximal aorta beginning at the end of the aortic sinus. The sections were stained with Oil-Red-O and counterstained with hematoxylin (Sigma-Aldrich), and quantitative analysis of lesions was performed on 15 sections from each animal (48). The remaining aortae were dissected out. *En face* preparations were longitudinally opened, pinned flat, stained with Sudan IV, photographed, and analyzed using the BIOQUANT true-color windows system (R&M Biometrics). The lesion was expressed as percentage of *en face* aorta surface. The analysis was performed by the same investigator blinded to the study groups.

Establishment of shRNA stable cell lines. We inserted 2 unique 19-bp oligos derived from 11βHSD2 mRNA, 5′-GGAGACAGGTAAGAAACTG-3′ and 5′-GGTGAACTTCTTTGGTGCA-3′, which targeted 11βHSD2 exon 2 and exon 3, as well as negative control, 5′-GCGCGCTTTGTAGGATTCG-3′ (Oligoengine), into pSuper.neo-GFP vector (Oligoengine), which provided the shRNA backbone and were named 11βHSD2/shRNA2, 11βHSD2/shRNA3, and shscramble, respectively. After sequence confirmation of each construct, we transfected 11βHSD2/shRNA2, 11βHSD2/shRNA3, and shscramble into subconfluent CT26 cells using Effectene (Qiagen) to produce stable cell lines designated CT26^{shRNA2}, CT26^{shRNA3}, and CT26^{shscramble}. After 24 h, DMEM containing 10% fetal bovine serum and 1 mg/ml G418 was used to select for G418-resistant clones. After 1 wk of G418-selective culture, the remaining cells were resuspended and reselected by fluorescence-activated cell sorting for the presence of GFP in the vector. Single clones were chosen by growing the reselected transfected cells under 1 mg/ml G418 using serial dilution.

Transient transfection of 11βHSD2. Expression vector pCMV-SPORT6, containing the entire open reading frame of mouse 11βHSD2 cDNA, was obtained from Open Biosystems. A total of 0.8 μg 11βHSD2 construct or empty pCMV-SPORTS vector was used for transient transfection into subconfluent CT26 cells using Effectene (Qiagen). The cells were used 48–72 h after transfection.

RNA isolation and quantitative real-time PCR. Total RNA was isolated from CT26 cells, stable cell lines, and human colonic adenomas and colon tissues using TRIzol reagents (Invitrogen) according to the manufacturer's instructions. Quantitative PCR was performed using the iCycler iQ Real Time PCR detection System (Bio-Rad). The primers used for mouse 11βHSD2 were 5′-GCCACTCTTGCGTCACTC-3′ (forward) and 5′-AGCCGAATGTGTCCATAAGC-3′ (reverse). The primers used for mouse GAPDH were 5′-CCAGAACATCATCCCTGCAT-3′ (forward) and 5′-GTTCAGCTCTGGGATGACCTT-3′ (reverse). The primers used for human 111βHSD2 (Hs00388669) and β-actin (Hs99999903) were from Applied Biosystems.

Cell migration and cell proliferation assays. CT26, HCA-7, and HT-29 cells were grown in DMEM supplemented with 4,500 mg/l glucose, 2 mM L-glutamine, 10% fetal bovine serum, 100 U/ml penicillin, and 100 μg/ml streptomycin in 5% CO_2 and 95% air at 37°C. Cell migration assays were performed in Transwells (8 μm; Corning Costar Co.) as previously described (49). The underside of each Transwell was precoated with collagen I overnight at 4°C, and the filter was subsequently blocked with 1% bovine serum albumin for 1 h at 37°C to inhibit nonspecific migration. CT26 cells were cultured in serum-free medium overnight and then treated with 10 μM GA, 10 nM CS, GA plus CS, or 10 μM of the COX-2 inhibitor SC58236 for 3 h. GA was added 30 min before addition of CS. The cell suspensions (100 μl, 1×10^6 cells/ml) were added to the wells, and cells were allowed to migrate into the matrix coated on the underside of the Transwell for 2.5 h. Cells on the top of the filter were removed, the filter was fixed in 4% formaldehyde and stained with 1% crystal violet, and migrating cells were counted using an image analysis system (R & M Biometrics). For cell proliferation assays, HCA-7 or HT-29 cells were cultured in 24-well plates (1 ml, 1×10^5 cells/well) in medium with or without the COX-2 inhibitors SC58236 (25 μM) or NS-398 (5 and 25 μM). The medium was changed every other day, and cells were counted 2, 4, and 6 d after seeding by an investigator blinded to the study groups.

Antibodies. Affinity-purified rabbit anti-mouse 11βHSD2 (catalog no. BHSD22-A) was purchased from Alpha Diagnostic International; rabbit anti-murine COX-2 (catalog no. 160106) and COX-1 (catalog no. 160109), rabbit anti-human mPGES-1 (catalog no. 160140) and cPGES (catalog no. 160150), and rabbit anti-rat 15-PGDH (catalog no. 160615) were from Cayman Chemicals; rabbit anti-human $cPLA_2$ (catalog no. 2382) and phosphorylated $cPLA_2$ (Ser505; catalog no. 2831) were from Cell Signaling; and goat anti-rat VEGF (catalog no. AF564) was from R&D Systems.

Preservation and fixation of mouse and human tissues. Tissues from human colonic adenoma resections were immersed in formalin and processed for paraffin embedding. The mice bearing tumors were anesthetized with Nembutal (60 mg/kg i.p.; Abbot Laboratories), given heparin (1,000 U/kg i.p.) to minimize coagulation, and perfused with fixative through the aortic trunk (15). After fixation, the tumor tissues were dehydrated, paraffin embedded, sectioned, and mounted on glass slides. The samples used in this study were from the Tennessee Colorectal Polyp Study (TCPS) protocol that was approved by the Institutional Review Board of Vanderbilt Medical Center, and written, informed consent was obtained from all participants.

Immunofluorescence/immunohistochemistry staining and quantitative image analysis. For immunofluorescence, frozen sections (without fixation) were first washed with PBS, then incubated with rat anti-murine CD31 antibody (BD Biosciences — Pharmingen) for 1 h and washed again with PBS. Washed sections were treated with fluorescence-conjugated secondary antibodies for 1 h. For paraffin-embedded tissue sections, the slides were deparaffinized, rehydrated, and stained with different antibodies, as previously described (15). Based on the distinctive density and color of immunostaining in video images, the number, size, and position of stained cells were quantified using the BIOQUANT true-color windows system (R & M Biometrics) as previously described (50).

Western blot analysis. Total CT26 cell lysate and total CT26 tumor lysate were used for Western blot analysis as described previously (51).

Measurement of prostanoids. Tumor PGE_2 levels were quantified by gas chromatographic/negative ion chemical ionization mass spectrometric assays using stable isotope dilution (52). PGE_2 concentration in the culture medium was measured using Prostaglandin E_2 Express EIA Kid according to the manufacturer's instruction (Cayman Chemical). The cells were first cultured in the medium with 10 nM CS. After 24 h, the medium was changed and incubated for an additional 1 h. The medium was collected for determination of PGE_2 concentration, and the cells were lysed for protein assay.

Mice received different concentrations of GA (3, 10, or 30 mg/kg) for 1 mo. Urinary excretion of the major murine PGI_2 and thromboxane metabolites (2,3-dinor-6-keto $PGF_{1\alpha}$ and 2,3-dinor thromboxane B_2, respectively) were measured by stable dilution isotope gas chromatography/mass spectrometry assays.

Measurement of CS, 11-keto-corticosterone, GA, and GE. At 24 h after the last i.p. injection of GA, the animals were sacrificed, and kidneys, colons, and tumors were collected and stored at –80°C. Tissue levels of CS, 11-keto-

corticosterone, GA, and GE were measured using high-performance liquid chromatography coupled with electrospray tandem mass spectrometry (53). GA and GE were from Sigma-Aldrich, CS was from ICN Biomedicals, and 11-keto-corticosterone was from Steroids.

To investigate the inhibition of CT26 cell 11βHSD2 activity by GA, cells were washed with serum-free medium, then treated with 100 nM CS alone or 100 nM CS plus 10 μM GA for 1 h, and medium was collected for determination of CS and 11-keto-corticosterone levels. GA was added 30 min before addition of CS. In the absence of any inhibitor, parental CT26 converted approximately 40% of the administered CS to the metabolite, 11-keto CS, indicating active 11βHSD2 activity in these cells. The inhibition of 11βHSD2 activity in CT26 by 11βHSD2 knockdown was also investigated using $CT26^{shRNA3-31}$ and $CT26^{shRNA2-9}$ cells. We expressed 11βHSD2 activity as timed production of 11-keto-corticosterone per mg protein.

Statistics. All values are presented as mean ± SD. Fisher exact test, ANOVA, and 2-tailed Student's *t* test with Bonferroni correction were used for statistical analysis. A *P* value less than 0.05 was considered significant.

Acknowledgments

This work was supported by American Cancer Society grant ACS-IRG-58-009-47 (to M.-Z. Zhang); by NIH grants DK39261 (to R.C. Harris and M.-Z. Zhang), DK62794 (to R.C. Harris), CA94849 and DK74359 (to A. Pozzi), DK48831 (to H. Yin), and CA97386 (to W. Zheng); and by funds from the Department of Veterans Affairs (to R.C. Harris). We thank Hui Cai, Yinghao Su, Guoliang Li, and Shiling Yang for their technical assistance.

Received for publication September 9, 2008, and accepted in revised form February 11, 2009.

Address correspondence to: Ming-Zhi Zhang, S-3223 MCN, Vanderbilt University Medical Center, Nashville, Tennessee 37232, USA. Phone: (615) 343-1548; Fax: (615) 343-2675; E-mail: ming-zhi.zhang@vanderbilt.edu. Or to: Raymond Harris, C3121 MCN, Vanderbilt University Medical Center, Nashville, Tennessee 37232, USA. Phone: (615) 322-2150; Fax: (615) 343-2675; E-mail: ray.harris@vanderbilt.edu.

1. Castellone, M.D., Teramoto, H., Williams, B.O., Druey, K.M., and Gutkind, J.S. 2005. Prostaglandin E2 promotes colon cancer cell growth through a Gs-axin-beta-catenin signaling axis. *Science.* **310**:1504–1510.
2. Steinbach, G., et al. 2000. The effect of celecoxib, a cyclooxygenase-2 inhibitor, in familial adenomatous polyposis. *N. Engl. J. Med.* **342**:1946–1952.
3. Baron, J.A., et al. 2003. A randomized trial of aspirin to prevent colorectal adenomas. *N. Engl. J. Med.* **348**:891–899.
4. Phillips, R.K., et al. 2002. A randomised, double blind, placebo controlled study of celecoxib, a selective cyclooxygenase 2 inhibitor, on duodenal polyposis in familial adenomatous polyposis. *Gut.* **50**:857–860.
5. Jacoby, R.F., Seibert, K., Cole, C.E., Kelloff, G., and Lubet, R.A. 2000. The cyclooxygenase-2 inhibitor celecoxib is a potent preventive and therapeutic agent in the min mouse model of adenomatous polyposis. *Cancer Res.* **60**:5040–5044.
6. Dannenberg, A.J., et al. 2001. Cyclooxygenase 2: a pharmacological target for the prevention of cancer. *Lancet Oncol.* **2**:544–551.
7. Gwyn, K., and Sinicrope, F.A. 2002. Chemoprevention of colorectal cancer. *Am. J. Gastroenterol.* **97**:13–21.
8. Bresalier, R.S., et al. 2005. Cardiovascular events associated with rofecoxib in a colorectal adenoma chemoprevention trial. *N. Engl. J. Med.* **352**:1092–1102.
9. Solomon, S.D., et al. 2005. Cardiovascular risk associated with celecoxib in a clinical trial for colorectal adenoma prevention. *N. Engl. J. Med.* **352**:1071–1080.
10. Stichtenoth, D.O., et al. 2001. Microsomal prostaglandin E synthase is regulated by proinflammatory cytokines and glucocorticoids in primary rheumatoid synovial cells. *J. Immunol.* **167**:469–474.
11. Zhang, M.Z., Harris, R.C., and McKanna, J.A. 1999. Regulation of cyclooxygenase-2 (COX-2) in rat renal cortex by adrenal glucocorticoids and mineralocorticoids. *Proc. Natl. Acad. Sci. U. S. A.* **96**:15280–15285.
12. Denis, M.G., Chadeneau, C., Blanchardie, P., and Lustenberger, P. 1992. Biological effects of glucocorticoid hormones on two rat colon adenocarcinoma cell lines. *J. Steroid Biochem. Mol. Biol.* **41**:739–745.
13. Dizon, D.S., and Kemeny, N.E. 2002. Intrahepatic arterial infusion of chemotherapy: clinical results. *Semin. Oncol.* **29**:126–135.
14. Schiffelers, R.M., et al. 2005. Liposome-encapsulated prednisolone phosphate inhibits growth of established tumors in mice. *Neoplasia.* **7**:118–127.
15. Zhang, M.Z., Hao, C.M., Breyer, M.D., Harris, R.C., and McKanna, J.A. 2002. Mineralocorticoid regulation of cyclooxygenase-2 expression in rat renal medulla. *Am. J. Physiol. Renal Physiol.* **283**:F509–F516.
16. Eberhart, C.E., et al. 1994. Up-regulation of cyclooxygenase 2 gene expression in human colorectal adenomas and adenocarcinomas. *Gastroenterology.* **107**:1183–1188.
17. Funder, J.W., Pearce, P.T., Smith, R., and Smith, A.I. 1988. Mineralocorticoid action: target tissue specificity is enzyme, not receptor, mediated. *Science.* **242**:583–585.
18. Yao, B., Harris, R.C., and Zhang, M.Z. 2005. Interactions between 11beta-hydroxysteroid dehydrogenase and COX-2 in kidney. *Am. J. Physiol. Regul. Integr. Comp. Physiol.* **288**:R1767–R1773.
19. Ikeda, K., et al. 2006. A long-term glycyrrhizin injection therapy reduces hepatocellular carcinogenesis rate in patients with interferon-resistant active chronic hepatitis C: a cohort study of 1249 patients. *Dig. Dis. Sci.* **51**:603–609.
20. Stormer, F.C., Reistad, R., and Alexander, J. 1993. Glycyrrhizic acid in liquorice--evaluation of health hazard. *Food Chem. Toxicol.* **31**:303–312.
21. Marandici, A., and Monder, C. 1993. Inhibition by glycyrrhetinic acid of rat tissue 11 beta-hydroxysteroid dehydrogenase in vivo. *Steroids.* **58**:153–156.
22. Sheng, H., et al. 1997. Inhibition of human colon cancer cell growth by selective inhibition of cyclooxygenase-2. *J. Clin. Invest.* **99**:2254–2259.
23. Yamazaki, R., Kusunoki, N., Matsuzaki, T., Hashimoto, S., and Kawai, S. 2002. Selective cyclooxygenase-2 inhibitors show a differential ability to inhibit proliferation and induce apoptosis of colon adenocarcinoma cells. *FEBS Lett.* **531**:278–284.
24. Tsujii, M., et al. 1998. Cyclooxygenase regulates angiogenesis induced by colon cancer cells. *Cell.* **93**:705–716.
25. Chen, X., et al. 2005. Increased plasma MMP9 in integrin alpha1-null mice enhances lung metastasis of colon carcinoma cells. *Int. J. Cancer.* **116**:52–61.
26. Bertagnolli, M.M., et al. 2006. Celecoxib for the prevention of sporadic colorectal adenomas. *N. Engl. J. Med.* **355**:873–884.
27. Cheng, Y., et al. 2002. Role of prostacyclin in the cardiovascular response to thromboxane A2. *Science.* **296**:539–541.
28. Pratico, D., Tillmann, C., Zhang, Z.B., Li, H., and FitzGerald, G.A. 2001. Acceleration of atherogenesis by COX-1-dependent prostanoid formation in low density lipoprotein receptor knockout mice. *Proc. Natl. Acad. Sci. U. S. A.* **98**:3358–3363.
29. Zhang, S.H., Reddick, R.L., Piedrahita, J.A., and Maeda, N. 1992. Spontaneous hypercholesterolemia and arterial lesions in mice lacking apolipoprotein E. *Science.* **258**:468–471.
30. Giovannucci, E., et al. 1995. Aspirin and the risk of colorectal cancer in women. *N. Engl. J. Med.* **333**:609–614.
31. Rosenberg, L., Louik, C., and Shapiro, S. 1998. Nonsteroidal antiinflammatory drug use and reduced risk of large bowel carcinoma. *Cancer.* **82**:2326–2333.
32. Thun, M.J., Namboodiri, M.M., and Heath, C.W., Jr. 1991. Aspirin use and reduced risk of fatal colon cancer. *N. Engl. J. Med.* **325**:1593–1596.
33. Miller, J.L. 1999. Decisions loom on selective COX-2 inhibitors. *Am. J. Health Syst. Pharm.* **56**:106–107.
34. Brown, J.R., and DuBois, R.N. 2005. COX-2: a molecular target for colorectal cancer prevention. *J. Clin. Oncol.* **23**:2840–2855.
35. Grosser, T., Fries, S., and FitzGerald, G.A. 2006. Biological basis for the cardiovascular consequences of COX-2 inhibition: therapeutic challenges and opportunities. *J. Clin. Invest.* **116**:4–15.
36. Moore, X.L., Hoong, I., and Cole, T.J. 2000. Expression of the 11beta-hydroxysteroid dehydrogenase 2 gene in the mouse. *Kidney Int.* **57**:1307–1312.
37. Clark, A.R., and Lasa, M. 2003. Crosstalk between glucocorticoids and mitogen-activated protein kinase signalling pathways. *Curr. Opin. Pharmacol.* **3**:404–411.
38. Rabbitt, E.H., et al. 2003. Abnormal expression of 11 beta-hydroxysteroid dehydrogenase type 2 in human pituitary adenomas: a prereceptor determinant of pituitary cell proliferation. *Oncogene.* **22**:1663–1667.
39. Rabbitt, E.H., Gittoes, N.J., Stewart, P.M., and Hewison, M. 2003. 11beta-hydroxysteroid dehydrogenases, cell proliferation and malignancy. *J. Steroid Biochem. Mol. Biol.* **85**:415–421.
40. Rabbitt, E.H., et al. 2002. Prereceptor regulation of glucocorticoid action by 11beta-hydroxysteroid dehydrogenase: a novel determinant of cell proliferation. *FASEB J.* **16**:36–44.
41. Lipka, C., et al. 2004. Impairment of the antiproliferative effect of glucocorticosteroids by 11beta-hydroxysteroid dehydrogenase type 2 overexpression in MCF-7 breast-cancer cells. *Horm. Metab. Res.* **36**:437–444.
42. Curreli, F., Friedman-Kien, A.E., and Flore, O. 2005. Glycyrrhizic acid alters Kaposi sarcoma-associated herpesvirus latency, triggering p53-mediated apoptosis in transformed B lymphocytes. *J. Clin. Invest.* **115**:642–652.
43. Backlund, M.G., et al. 2005. 15-Hydroxyprostaglandin dehydrogenase is down-regulated in colorectal cancer. *J. Biol. Chem.* **280**:3217–3223.
44. Tong, M., and Tai, H.H. 2005. 15-Hydroxyprostaglandin dehydrogenase can be induced by dexa-

methasone and other glucocorticoids at the therapeutic level in A549 human lung adenocarcinoma cells. *Arch. Biochem. Biophys.* **435**:50–55.
45. van Gelderen, C.E., Bijlsma, J.A., van Dokkum, W., and Savelkoul, T.J. 2000. Glycyrrhizic acid: the assessment of a no effect level. *Hum. Exp. Toxicol.* **19**:434–439.
46. Pozzi, A., et al. 2004. Colon carcinoma cell growth is associated with prostaglandin E2/EP4 receptor-evoked ERK activation. *J. Biol. Chem.* **279**:29797–29804.
47. Wang, J., et al. 1995. Demonstration that mutation of the type II transforming growth factor beta receptor inactivates its tumor suppressor activity in replication error-positive colon carcinoma cells. *J. Biol. Chem.* **270**:22044–22049.
48. Belton, O.A., Duffy, A., Toomey, S., and Fitzgerald, D.J. 2003. Cyclooxygenase isoforms and platelet vessel wall interactions in the apolipoprotein E knockout mouse model of atherosclerosis. *Circulation.* **108**:3017–3023.
49. Sheng, H., Shao, J., Washington, M.K., and DuBois, R.N. 2001. Prostaglandin E2 increases growth and motility of colorectal carcinoma cells. *J. Biol. Chem.* **276**:18075–18081.
50. Zhang, M.Z., et al. 2006. Renal cortical cyclooxygenase 2 expression is differentially regulated by angiotensin II AT(1) and AT(2) receptors. *Proc. Natl. Acad. Sci. U. S. A.* **103**:16045–16050.
51. Harris, R.C., Zhang, M.Z., and Cheng, H.F. 2004. Cyclooxygenase-2 and the renal renin-angiotensin system. *Acta Physiol. Scand.* **181**:543–547.
52. Coffey, R.J., et al. 1997. Epidermal growth factor receptor activation induces nuclear targeting of cyclooxygenase-2, basolateral release of prostaglandins, and mitogenesis in polarizing colon cancer cells. *Proc. Natl. Acad. Sci. U. S. A.* **94**:657–662.
53. Brady, A.E., et al. 2008. Centrally active allosteric potentiators of the M4 muscarinic acetylcholine receptor reverse amphetamine-induced hyperlocomotor activity in rats. *J. Pharmacol. Exp. Ther.* **327**:941–953.